Chem. Res. Toxicol., 21(4):888-894, 2008.
doi: 10.1021/tx7003213

Quartz inhibits glucose 6-phosphate dehydrogenase in murine alveolar macrophages.

Manuela Polimeni[†#1], *Elena Gazzano*[†#1], *Mara Ghiazza*[‡#], *Ivana Fenoglio*[‡#], *Amalia Bosia*[†#], *Bice Fubini*[‡#], *Dario Ghigo*[†#*]

[†]Dipartimento di Genetica, Biologia e Biochimica, Università di Torino, Via Santena 5/bis, Italy

[‡]Dipartimento di Chimica IFM, Università di Torino, Via P. Giuria 7, Italy

[#]Interdepartmental Center "G. Scansetti" for Studies on Asbestos and Other Toxic Particulates, Università di Torino, Italy

[*]AUTHOR EMAIL ADDRESS: dario.ghigo@unito.it

TITLE RUNNING HEAD: Quartz inhibits glucose 6-phosphate dehydrogenase

CORRESPONDING AUTHOR FOOTNOTE: Dario Ghigo, Dipartimento di Genetica, Biologia e Biochimica - Sezione di Biochimica, Via Santena, 5/bis - 10126 Torino – Italy, tel. +39-011-6705849 - fax +39-011-6705845, e-mail: dario.ghigo@unito.it

Table of Contents Graphic.

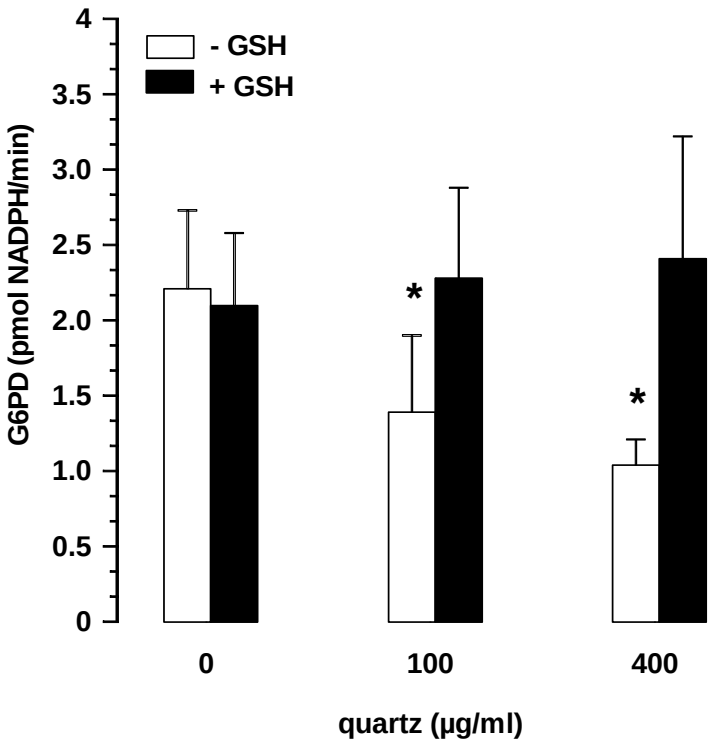

ABSTRACT. Crystalline silica is well known to induce an oxidative stress as a consequence of both surface-derived generation of free radicals and intracellular production of reactive oxygen species upon phagocytosis, the mechanism of the latter being still partially unknown. In this study we report that, in murine alveolar MH-S macrophages, a 24 h incubation with quartz particles (80 μg/cm^2) inhibits the glucose 6-phosphate dehydrogenase (G6PD)[2] activity by 70% and the pentose phosphate pathway by 30%. Such effects are accompanied by the 50% decrease of intracellular glutathione, a 35% increase of thiobarbituric acid-reactive products (index of lipoperoxidation) and a five-fold increase of leakage of lactate dehydrogenase in the extracellular medium (index of cytotoxicity). Quartz inhibits G6PD but not other oxidoreductases, and such inhibition is fully prevented by glutathione, suggesting that silica exerts on G6PD an oxidative damage. Our data provide a new additional mechanism by which silica may induce oxidative stress, i.e. by inhibiting the pentose phosphate pathway, one of the main antioxidant metabolic pathways of the cell.

FOOTNOTES

[1]Manuela Polimeni and Elena Gazzano contributed equally to this work.

[2]Abbreviations: 6PGD, 6-phosphogluconate dehydrogenase; G6PD, glucose 6-phosphate dehydrogenase; GSH, glutathione; GSSG, glutathione disulfide; LDH, lactate dehydrogenase; PPP, pentose phosphate pathway; ROS, reactive oxygen species; RT-PCR, reverse transcriptase-polymerase chain reaction; TBARS, thiobarbituric acid reactive substances.

INTRODUCTION

Inhalation of crystalline silica has been associated with several diseases including silicosis, chronic obstructive pulmonary disease, emphysema, bronchogenic carcinoma, chronic renal diseases and other autoimmune diseases (*1-3*). Although the pathogenetic mechanisms are still far from being completely understood, it is widely acknowledged that the inflammatory and toxic effects of silica are exerted via the generation of reactive oxygen species (ROS), having two main sources: the generation of free radicals at the particle surface and the production of ROS by silica-activated phagocytes (*1-3*). Silica has been reported to deplete some antioxidant defences in the lung such as ascorbic acid and glutathione (*4*). The subsequent oxidative stress can result in activation of cell signaling pathways, increased expression of specific transcription factors and inflammatory cytokines, apoptosis, genotoxic effects and cell transformation (*2,3,5*). Yet, the cellular mechanisms responsible for the increased ROS generation are still obscure.

The pentose phosphate pathway (PPP) is one of the metabolic pathways most sensitive to a cell oxidative stress: in the PPP oxidative phase, glucose 6-phosphate is irreversibly converted into ribulose 5-phosphate and CO_2, leading to the synthesis of NADPH, a redox cofactor for many antioxidant enzymes. Glucose 6-phosphate dehydrogenase (G6PD) catalyzes the first and rate-limiting step of the pathway, and is mainly regulated by the NADPH/$NADP^+$ ratio. Any oxidative stress causes a decrease of this ratio, which in turn activates G6PD activity and PPP. Thus the metabolic flux through PPP represents a very sensitive index of the cell exposure to oxidant molecules. To our knowledge, no measurement of PPP flux has been reported until now in cells exposed to silica particles. When investigating the effects of pure crystalline silica (quartz) on the PPP in murine alveolar macrophages, quite surprisingly we observed no short-term activation of PPP after 1 h of incubation: on the contrary, silica caused a clear inhibition of this pathway after a 24 h incubation. Starting from this observation, we have performed this experimental work, aimed to clarify the cause of PPP inhibition, which may represent a novel mechanism of oxidative stress in silica-exposed cells, since a decrease of the reducing power may impair the cell ability to oppose ROS generation.

EXPERIMENTAL PROCEDURES

Materials. The silica sample was pure quartz powder (1-10 μm diameter range) obtained by grinding a very pure quartz crystal (Madagascar quartz) in a planetary ball mill (S1 50 Hz; Retsch GmbH, Haan, Germany) for 3 h and then in a mixer mill for 9 h (MM200 27 Hz; Retsch GmbH) by using agate jar and balls in order to avoid any contamination by metals. When not otherwise specified, reagents were from Sigma-Aldrich S.r.l. (Milan, Italy). Menadione was dissolved in dimethylsulfoxide; in each experimental condition, controls and the other samples received the same volume addition of solvent, the final concentration of which never exceeded 0.2%.

Cells. Murine alveolar macrophages (MH-S), provided by Istituto Zooprofilattico Sperimentale "Bruno Ubertini" (Brescia, Italy), were cultured in 35 or 100 mm-diameter Petri dishes in RPMI-1640 + 10% FBS up to 90% confluence, and then incubated in the same culture medium for 24 h in the absence or presence of silica before the assays. The protein content of the cell monolayers, cell suspensions and cell lysates was assessed with the BCA kit from Pierce (Rockford, IL). Each result obtained from cell cultures, suspensions or lysates was related to the amount of cellular proteins in the same sample.

Measurement of extracellular LDH activity. The cytotoxic effect of quartz was measured as leakage of lactate dehydrogenase (LDH) activity into the extracellular medium (*6,7*). After each incubation the extracellular medium was collected and centrifuged at 13,000 x g for 30 min. The cells (cultured in 35 mm-diameter Petri dishes) were washed with fresh medium, detached with trypsin/EDTA (0.05/0.02% v/v), washed with PBS, resuspended in 1 ml of TRAP (triethanolamine 82.3 mM, pH 7.6), and sonicated on ice with two 10-s bursts. Aliquots of cell lysate (5 μl) and of extracellular medium (50 μl) were diluted with TRAP and supplemented with sodium pyruvate 0.5 mM and NADH 0.25 mM (final volume of the mix: 300 μl) to start the reaction. The reaction was followed for 10 min, measuring the absorbance at 340 nm (37°C) with a Packard EL340 microplate reader (Bio-Tek Instruments, Winooski, VT). Each reaction kinetics was linear throughout the time of measurement. Both intracellular and extracellular enzyme activity was expressed as μmol of NADH

oxidized/min/dish, then extracellular LDH activity (LDH out) was calculated as percentage of the total (intracellular + extracellular) LDH activity (LDH tot) in the dish.

Measurement of thiobarbituric acid reactive substances (TBARS). TBARS assay, used as a screening method for lipid peroxidation, was performed according to Yano (*8*). After a 24 h incubation in the absence or presence of pure quartz, the cells (cultured in 35 mm-diameter Petri dishes) were washed with fresh medium, detached with trypsin/EDTA, and resuspended in 1 ml of PBS. Aliquots of 500 µl of cellular suspension, each containing the same protein amount (0.1 mg), were added to 5 µl of Triton X-100 and 500 µl of TBA solution (0.375% thiobarbituric acid and 30% trichloroacetic acid in 0.5 N HCl). Samples were boiled for 20 min, rapidly cooled by immersion in an ice bath and centrifuged for 30 s at 13,000 x g. The absorbance of 300 µl of the reaction mixture was read at 532 nm with a Packard EL340 microplate reader. TBARS values were expressed as pmol/mg cellular protein.

Detection of apoptosis. After a 24 h incubation in the absence or presence of quartz, the cells (cultured in 35 mm-diameter Petri dishes) were washed with PBS, detached with trypsin/EDTA, added to floating cells previously collected from the supernatant and resuspended at 3 x 10^5 cells/0.5 ml of binding buffer (containing 10 mM Hepes, 2.5 mM $CaCl_2$, 140 mM NaCl, pH 7.4). These cell suspensions were incubated for 10 min with 25 µg propidium iodide (PI, Calbiochem-Novabiochem Corporation, La Jolla, CA) and 5 µl annexin V-FITC (0.05 mg/ml). Cells were washed and fluorescence was measured at 488 nm (excitation)-530 nm (emission) for annexin V or 536 nm (excitation)-617 nm (emission) for PI detection, using a Perkin-Elmer LS-5 fluorimeter (Perkin Elmer, Shelton, CT). Results were expressed as average percentage values obtained from triplicate experiments versus controls.

Measurement of pentose phosphate pathway (PPP) activity. The metabolic fluxes through the PPP and the tricarboxylic acid cycle were measured, as previously described (*6*), by detecting the amount of $^{14}CO_2$ developed from [^{14}C]glucose (Dupont-New England Nuclear, Boston, MA) in 1 h. After a 3, 6 or 24 h incubation in the absence or presence of 20 or 80 µg/cm^2 quartz particles, cells (cultured in 100 mm-diameter Petri dishes) were washed with fresh medium, detached with trypsin/EDTA, washed with PBS, and resuspended in 1 ml of Hepes buffer (in mM: 145 NaCl, 5 KCl, 1 $MgSO_4$, 10 Hepes sodium

salt, 10 glucose, 1 $CaCl_2$, pH 7.4, at 37 °C) containing 2 μCi of [1-^{14}C]glucose or [6-^{14}C]glucose (58 and 55 mCi/mmol, respectively; Dupont-New England Nuclear, Boston, MA). The cell suspensions, containing 0.5 mg of cell proteins (corresponding to about 250,000 cells) in 1 ml, were then incubated for 1 h in the absence or presence of particulate or 100 μM menadione (as a control oxidative stress), using a closed experimental system to trap the $^{14}CO_2$ developed from [^{14}C]glucose, as detailed previously (*6*). We measured also the PPP and the tricarboxylic acid cycle after a 1 h incubation with particulate: in this case, due to the shorter time, the incubation of the cells with silica was performed during the 1 h of $^{14}CO_2$ development in the closed system. This direct incubation of silica with cells in the experimental system is not possible for longer time periods, owing to the poor viability of cells suspended in Hepes buffer for more than 1-2 h. The PPP metabolic flux (expressed as pmol CO_2/h/mg cell proteins) was obtained by subtracting the amount of CO_2 developed from [6-^{14}C]glucose from the CO_2 released from [1-^{14}C]glucose. The extent of [6-^{14}C]glucose metabolism, an index of the tricarboxylic acid cycle alone, did not change significantly in the different experimental conditions (not shown).

Measurement of G6PD and 6-phosphogluconate dehydrogenase (6PGD) activities. After a 24 h incubation in the absence or presence of particulate, the cells (cultured in 35 mm-diameter Petri dishes) were washed with fresh medium, detached with trypsin/EDTA, washed with PBS, resuspended in 0.1 M Tris, 0.5 mM EDTA, pH 8.0, and sonicated on ice with two 10-s bursts. The cell lysate was supplemented with 10 mM $MgCl_2$ and 0.25 mM $NADP^+$, and each measurement was performed on 1 ml of this reaction mix. The reaction was started at 37 °C by adding 6-phosphogluconate (0.6 mM) with or without glucose 6-phosphate (0.6 mM) and measured in a Lambda 3 spectrophotometer (Perkin Elmer) as the increase of absorbance/min at 340 nm (*6*). The most commonly used assays for G6PD activity measure the rate of reduction of $NADP^+$ to NADPH when a cell lysate is incubated with glucose 6-phosphate. However, the product of G6PD activity, 6-phosphogluconate, is largely oxidized further in the 6-phosphogluconate dehydrogenase (6PGD) reaction so that more than 1 (nearly 2) mole of $NADP^+$ is reduced per each mole of glucose 6-phosphate oxidized. The assay results can be corrected for the

6PGD-mediated oxidation as follows. A first measurement is performed by adding to the assay system a saturating amount of both 6-phosphogluconate and glucose 6-phosphate; the rate of $NADP^+$ reduction is the result of both G6PD and 6PGD activities. A second assay is performed with 6-phosphogluconate only as a substrate; this procedure allows us to measure 6PGD activity alone. G6PD activity is obtained by subtracting the rate of the second assay from the rate of the first one (*6*). Enzymatic activity was expressed as pmol of $NADP^+$ reduced/min/mg of cell proteins. Each reaction kinetics was linear throughout the 20 min of observation.

Measurement of glyceraldehyde 3-phosphate dehydrogenase (GAPDH) activity. Cells (cultured in 35 mm-diameter Petri dishes) were washed with fresh medium, detached with trypsin/EDTA, washed with PBS, resuspended in 300 µl of 0.1 M Tris, 0.5 mM EDTA, pH 8.0, and sonicated on ice with two 10-s bursts. The cell lysate was then diluted to a final volume of 1 ml with the same Tris/EDTA buffer supplemented with (final concentrations): 1.1 mM ATP, 0.1 mM NADH, 0.9 mM EDTA, 2 mM $MgSO_4$, 3-phosphoglycerate kinase (4 U/ml). The reaction was started at 37 °C by adding 3-phosphoglyceric acid (3.72 mM) and the absorbance change was measured at 340 nm in a Lambda 3 spectrophotometer as previously described (*6*). Enzymatic activity was expressed as µmol of NADH oxidized/min/mg of cell proteins. Each reaction kinetics was linear throughout the 20 min of observation.

Measurement of enzyme activities in cell-free experiments. Purified G6PD (2 U) (from *S. cerevisiae*, purity > 99.5%, Sigma-Aldrich), purified GAPDH (20 U) (from rabbit muscle, purity > 99.5%, Sigma-Aldrich), or purified LDH (100 U) (from bovine muscle, purity > 99.5%, Sigma-Aldrich) were incubated at 37 °C in 1 ml of 0.1 M Tris pH 8.0, in the absence or presence of 100 or 400 µg/ml quartz (concentrations corresponding respectively to 20 and 80 $\mu g/cm^2$ in the culture dishes) and 50 µM GSH. In these tests we chose the concentrations of purified enzymes exhibiting kinetics similar to those observed in the cell lysates. After a 4 h incubation the suspension was centrifuged at 13,000 x g for 5 min in a refrigerated microcentrifuge to spin down the silica particles. Each enzyme activity was

measured spectrophotometrically in the supernatant, using a Lambda 3 spectrophotometer as previously described (*6*).

G6PD expression. Total RNA was obtained by the guanidinium thiocyanate-phenol-chloroform method (*9*). Three µg of total RNA were reversely transcribed into cDNA at 37°C for 50 min, using 1 µl oligo $(dT)_{12-18}$ (500 µg/ml) and 50 U/µl M-MLV reverse transcriptase (Invitrogen, Paisley, UK). The reverse transcription was carried out in a total volume of 40 µl, according to the manufacturer's recommendations. The reverse transcriptase-polymerase chain reaction (RT-PCR) efficiency was checked by amplifying a β-actin fragment, used as housekeeping control gene. cDNA products were determined by PCR amplification, carried out in a total volume of 50 µl with the Eurotaq PCR Kit (Euroclone, Pero, Italy), according to the manufacturer's recommendations. Primers for G6PD were: 5′-CCGGATCGACCACTACCTGGGCAAG-3′, 5′-GTTCCCCACGTACTGGCCCAGGACCA-3′ (343 bp); primers for β-actin were: 5′-GGTCATCTTCTCGCGGTTGGCCTTGGGGT-3′, 5′-CCCCAGGCACCAGGGCGTGAT-3′ (230 bp). PCR amplification for G6PD was performed as follows: 1 cycle of denaturation at 95°C for 15 min, 35 cycles of denaturation at 94°C for 1 min, annealing at 56°C for 1 min, elongation at 72°C for 2 min, and 1 cycle of extension at 72°C for 5 min. PCR amplification for β-actin was performed as follows: 1 cycle of denaturation at 95°C for 8 min, 32 cycles of denaturation at 94°C for 30 s, annealing at 54°C for 30 s, elongation at 72°C for 1 min, and 1 cycle of extension at 72°C for 7 min. Samples were electrophoresed in 1% agarose gels containing ethidium bromide in Tris-acetate/EDTA buffer to visualize the PCR products.

Measurement of glutathione. Glutathione (GSH) and glutathione disulfide (GSSG) were measured as previously described (*10*), using a modified glutathione reductase-DTNB recycling assay. The cells (cultured in 35 mm-diameter Petri dishes) were washed with PBS and 600 µl 0.01 N HCl were added to each cell monolayer. After gentle scraping, the cells were frozen/thawed twice and the proteins were precipitated by adding 120 µl of 6.5% 5-sulfosalicylic acid to 480 µl of lysate. Each sample was placed in ice for 1 h and centrifuged for 15 min at 12,500 x g (4°C). The total glutathione was measured in 20 µl of the cell lysate with the following reaction mix: 20 µl stock buffer (143 mM NaH_2PO_4, 63 mM

EDTA, pH 7.4), 200 µl daily reagent [10 mM 5,5'-dithiobis-2-nitrobenzoic acid (DTNB), 2 mM NADPH in stock buffer], 40 µl glutathione reductase (8.5 U/ml). The content of GSSG was obtained after derivatization of GSH with 2-vinylpyridine (2VP): 10 µl of 2VP were added to 200 µl of cell lysate and the mixture was shaken at room temperature for 1 h. Glutathione was then measured in 40 µl of sample as described. The kinetics of reaction was followed at 415 nm for 10 min (to check it was linear) using a Packard microplate reader EL340. Each measurement was made in triplicate and results were expressed as nmol of glutathione/mg cellular protein. For each sample, GSH was obtained by subtracting GSSG from total glutathione.

Statistical analysis. All data in text and figures are provided as means ± SD. The results were analyzed by a one-way Analysis of Variance (ANOVA) and Tukey's test. $p < 0.05$ was considered significant.

RESULTS

A 24 h incubation with pure quartz induced in MH-S cells a concentration-dependent cytotoxic effect, measured as leakage of intracellular LDH activity into the extracellular medium (Fig. 1A). We tested also 100 and 150 μg/cm^2 quartz, but these concentrations were too toxic (not shown). Under the same experimental conditions, a significantly increased production of lipid peroxidation markers (TBARS) was detectable after the incubation with 80 μg/cm^2 quartz but not at lower concentrations (Fig. 1B). In the light of these preliminary data, we decided to use in the subsequent experiments the concentrations 20 and 80 μg/cm^2, because the former was the lowest one able to exert a significant cytotoxic effect and the latter was the lowest concentration able to increase significantly the markers of lipid peroxidation.

LDH is a soluble cytosolic enzyme that is released into the culture medium following loss of membrane integrity resulting from either apoptosis or necrosis. To determine whether the exposure to silica resulted in apoptotic death, after a 24 h incubation with quartz we stained the cells with annexin V-FITC and PI (*11)*. When MH-S cells were incubated with 20 μg/cm^2 quartz, only the amount of annexin V-FITC-positive cells, an index of early apoptosis, increased significantly; after the incubation with 80 μg/cm^2 quartz the amount of annexin V-FITC-positive cells increased further and that of PI-positive cells was significantly increased (Fig. 2). The cell staining with PI is an index of late apoptosis or death (*11)*. Taken as a whole, these data suggest that, after a 24 h incubation with 20-80 μg/cm^2 quartz, the majority of damaged MH-S cells was apoptotic.

Experiments performed with pure quartz at the concentrations 20 and 80 μg/cm^2 showed that silica did not significantly change the PPP after a 1, 3 and 6 h incubation with MH-S cells, if compared to control cells (Fig. 3A). The PPP was significantly inhibited only after a 24 h incubation with 80 μg/cm^2 quartz (Fig. 3A). The same phenomenon was observed when we measured the effect of quartz on the PPP activity stimulated by menadione (Fig. 3B), a compound which exerts an oxidative stress by generating superoxide anion through its redox cycling and by forming a conjugate with glutathione (*12*). Menadione-stimulated PPP activity is an useful index of maximal activation of the pathway and therefore of the antioxidant potential of PPP. The PPP flux is mainly regulated by the activity of G6PD:

similarly to PPP experiments, a 24 h incubation of the cells with quartz significantly inhibited the G6PD activity at 80 μg/cm^2 but not at the lower concentration (Fig. 4). The activity of another oxidoreductase of the same pathway, 6PGD, was not significantly modified at either quartz concentration in comparison with controls.

The RT-PCR experiments showed that, after a 24 h incubation with 20 or 80 μg/cm^2 quartz, the expression of G6PD mRNA in MH-S cells was not significantly modified in comparison with controls (not shown). To check whether silica particles could directly inhibit G6PD, we incubated for 4 h the cell lysate in the absence or presence of either 100 or 400 μg/ml quartz (concentrations corresponding respectively to 20 and 80 μg/cm^2 in the culture dishes) and then the residual enzyme activity was measured as previously described (*6*). After a 4 h incubation with either 100 or 400 μg/ml quartz, G6PD activity was significantly inhibited when compared to the control (Fig. 5). On the other hand, the activity of 6PGD was not significantly modified by a 4 h incubation of the cell lysate with both quartz concentrations under the same experimental conditions (Fig. 5). When the cell lysate was incubated for 4 h in the presence of both 0.5 mM GSH and either 100 or 400 μg/ml quartz, the G6PD inhibition exerted by quartz was completely prevented in comparison with the lysate incubated with GSH alone (Fig. 5).

To provide stronger evidence that quartz directly influences the G6PD activity, we incubated the purified enzyme in the absence or presence of either 100 or 400 μg/ml quartz, and the residual enzyme activity was measured after 4 h (Fig. 6). Both silica concentrations significantly decreased the G6PD activity in cell-free conditions. Again, such inhibition was prevented when G6PD was incubated with quartz in the presence of 0.5 mM GSH (which per se did not significantly modify the enzyme activity) (Fig. 6).

On the contrary, the activities of GAPDH and LDH were not significantly changed by a 4 h incubation of the cell lysates with quartz (100 and 400 μg/ml) (Fig. 7). Similarly, the activities of purified GAPDH and LDH were not inhibited after a 4 h incubation with quartz in cell-free conditions (Fig. 7).

After a 24 h incubation with MH-S cells, 80 μg/cm^2 quartz significantly decreased the intracellular level of GSH and increased the intracellular GSSG (Fig. 8). The ability of 20 μg/cm^2 quartz to induce LDH release without eliciting signs of oxidative damage and PPP inhibition may suggest that either the lower concentration of quartz can exert toxic effects, via different surface characteristics, not dependent on oxidative damage as previously reported by Bruch et al. (*13*), or that the LDH measurement is a test more sensitive than those used to detect the oxidative stress.

DISCUSSION

While the mechanisms of free radical generation at the surface of silica particles have been intensively investigated (*14,15*), the biochemical source of ROS in silica-exposed cells is far from being clarified. A greater knowledge of such topics is particularly important in the prevention of silica-associated pathologies, since ROS are universally acknowledged to be the main effectors of cytotoxic (*16*), genotoxic (*17*) and transforming effects (*18*) of silica. The cellular generation of ROS is considered to be a consequence of the increase in oxygen consumption, called "respiratory burst", which is triggered in macrophages/neutrophils in response to phagocytosis of microorganisms and particulates (*2*). But the evidences that NAD(P)H oxidases mediate the production of ROS in silica-exposed cells are indirect, based only on enzyme inhibitory studies using diphenylene iodonium (*19-21*), which is not a specific inhibitor of NAD(P)H oxidases (*22*). Thus, although silica is considered an activator of respiratory burst, no direct evidence of the involvement of specific metabolic pathways in ROS generation is available. Furthermore, an oxidative stress or an oxidative burst should elicit the activation of PPP, which produces the NADPH necessary to keep glutathione in the reduced form and to provide NADPH oxidase with reducing equivalents. Instead, such a PPP activation is not observed in cells incubated with silica. On the contrary, a 24 h incubation with quartz decreases the cell ability to activate PPP in response to an oxidative stress, and a parallel increase of the signs of GSH consumption (lower GSH/GSSG ratio), lipoperoxidation (TBARS accumulation) and cytotoxicity (higher leakage of LDH into the extracellular medium) can be observed. The PPP flux is regulated by the activity of G6PD, which catalyzes the first and rate-limiting step of the pathway: for this reason, PPP can be considered a sensitive index of the actual G6PD activity in a whole cell. We investigated the G6PD activity in the cell lysate, which, being measured in the presence of saturating concentrations of substrate, provides information about the maximal enzyme activity, i.e. about the cell content of active enzyme molecules. G6PD activity was, as well as PPP, significantly diminished; this inhibition was specific, as the activity of 6PGD, another PPP enzyme producing NADPH, did not change significantly.

A decrease of G6PD activity might be attributable to a diminished expression or to a permanent modification of the enzyme. The former hypothesis was ruled out by RT-PCR experiments, which did not show significant differences of the G6PD mRNA transcription in cells incubated in the presence or absence of silica. We then hypothesized a direct effect of silica particles on G6PD: indeed, in vivo, after phagocytosis, the particles may enter into close contact with cytosolic enzymes. To mimic this situation we incubated the quartz particles with the cell lysates of MH-S cells, and checked the activity of four different oxidoreductases: after such incubation, G6PD was significantly inhibited, while the activity of 6PGD, LDH and GAPDH did not differ from that detected in the cell lysate alone. When purified G6PD, LDH and GAPDH were incubated with quartz in cell-free conditions, only G6PD was significantly inhibited. This result rules out that the inhibitory effect of quartz is exerted aspecifically on every kind of NAD(P)-dependent enzyme.

Comparing the effects of quartz on PPP flux and G6PD activity shown in figures 3 and 4, it can be observed that at the higher concentration the G6PD inhibition was more prominent than the decrease of PPP activity. This discrepancy can be accounted for by the different measurement procedures. PPP flux is strictly related to the in vivo G6PD activity, and is measured at the intracellular concentrations of reagents, which are low and not saturating, so that the G6PD rate is far from Vmax. G6PD activity is measured in lysed cells in the presence of saturating concentrations of reagents, then the enzyme rate matches the Vmax. Furthermore, G6PD has been demonstrated to operate normally at a rate that is a small fraction (0.05-2%) of its Vmax (*23*): this so called "restraint" is a common feature of G6PD from all somatic cells. When cells are lysed to measure G6PD Vmax, the restraining factors are removed, unmasking a vast reserve of enzyme activity. For these reasons, the changes of PPP flux in whole cells (an index of actual G6PD activity) may not match quantitatively those of G6PD Vmax measured on the cell lysate (an index of the maximal enzyme activity), and this could account for the observation that G6PD and PPP are inhibited by the particles to different extents.

Quartz is likely to inhibit the G6PD activity via an oxidative mechanism: indeed GSH protected G6PD from silica-induced inhibition in the experiments performed on cell lysates. G6PD is known to

contain several cysteines, and some of them are important for enzyme activity, because thiol group inhibitors exert a marked inhibition (*24*). Taken as a whole, our data suggest that silica particles inhibit G6PD via an oxidative damage, and the subsequent decrease of PPP flow could make the cell unable to recover the normal GSH/GSSG ratio, which is directly lowered by silica. Increased consumption of GSH and decreased ability to regenerate the reduced cofactor could in turn trigger a vicious circle, allowing a further oxidative damage of G6PD and a cell injury. Thus, silica-exposed cells would be less able to counteract the oxidative stress generated by particles themselves and by other oxidizing agents, such as menadione or physiological derivatives of redox metabolism: indeed, each day about 2% of oxygen consumed by human tissues is incompletely reduced to ROS (*25*). The reduced ability to neutralize ROS could partly account for the increased signs of oxidative stress observed both in vitro and in vivo after silica exposure (*3*).

It is interesting to observe that several silicates, i.e. asbestos mineral fibers such as crocidolite (*6*), chrysotile (*26*) and amosite (*27*) exhibited the same ability to inhibit G6PD and PPP activity in human lung epithelial cells A549, while glass fibers MMVF10 were devoid of this effect (*6*). Asbestos silicates contain variable amounts of metals, particularly iron, which has been heavily implicated in the pathogenic effects of asbestos (*28*). The quartz sample we used is a much more pure material, a SiO_2 form virtually devoid of metals. Thus iron is not likely to be the main responsible for the oxidative stress exerted by quartz in our experiments. Experiments with pure quartz and iron-deprived quartz dusts have already shown that hydroxyl radicals can be generated in the absence of trace iron at the crystal surface (*29*). We think that our data suggest a new mechanism of silica-evoked oxidative stress, wherein particles induce oxidative stress also by inhibiting one of the main antioxidant pathways of the cell. This mechanism would offer a unifying basis for several common cytotoxic aspects which are exhibited by both asbestos and silica. Our future efforts are aimed to compare these effects of pure quartz to those of other silica particles differing as far as size, composition and surface reactivity are concerned, in order to understand the mechanism by which silica alters the cellular redox metabolism, triggering the chain of events leading to cell death or transformation.

ACKNOWLEDGMENTS

The research has been carried out with the financial support of MIUR and University of Torino (Funds for Selected Research Topics).

REFERENCES

1. Mossman, B.T., and Churg, A. (1998) Mechanisms in the pathogenesis of asbestosis and silicosis. *Am. J. Respir. Crit. Care Med. 22*, 1666-1680.

2. Ding, M., Chen, F., Shi, X., Yucesoy, B., Mossman, B., and Vallyathan, V. (2002) Diseases caused by silica: mechanisms of injury and disease development. *Int. Immunopharmacol. 2*, 173-182.

3. Fubini, B., and Hubbard, A. (2003) Reactive oxygen species (ROS) and reactive nitrogen species (RNS) generation by silica in inflammation and fibrosis. *Free Radic. Biol. Med. 34*, 1507-1516.

4. Brown, D.M., Beswick, P.H., Bell, K.S., and Donaldson, K. (2000) Depletion of glutathione and ascorbate in lung lining fluid by respirable fibres. *Ann. Occup. Hyg. 44*, 101-108.

5. Castranova, V. (2004) Signaling pathways controlling the production of inflammatory mediators in response to crystalline silica exposure: role of reactive oxygen/nitrogen species. *Free Radic. Biol. Med. 37*, 916-925.

6. Riganti, C., Aldieri, E., Bergandi, L., Fenoglio, I., Costamagna, C., Fubini, B., Bosia, A., and Ghigo, D. (2002) Crocidolite asbestos inhibits pentose phosphate pathway and glucose 6-phospate dehydrogenase activity in human lung epithelial cells. *Free Radic. Biol. Med. 32*, 938-949.

7. Kinnula, V.L., Aalto, K., Raivio, K.O., Walles, S., and Linnainmaa, K. (1994) Cytotoxicity of oxidants and asbestos fibers in cultured human mesothelial cells. *Free Radic. Biol. Med. 16*, 169-176.

8. Yano, E. (1988) Mineral fiber-induced malondialdehyde formation and effects of oxidant scavengers in phagocytic cells. *Int. Arch. Occup. Environ. Health 61*, 19-23.

9. Chomczynski, P., and Sacchi, N. (1987) Single-step method of RNA isolation by acid guanidinium thiocyanate–phenol–chloroform extraction. *Anal. Biochem. 162*, 156-159.

10. Vandeputte, C., Guizon, I., Genestie-denis, I., Vannier, B., and Lorenzon, G. (1994) A microtiter assay for total glutathione and glutathione disulfide contents in cultured/isolated cells: performance study of a new miniaturized protocol. *Cell Biol. Toxicol. 10*, 415-421.

11. Kanupriya, Prasad, D., Sai Ram, M., Sawhney, R.C., Ilavazhagan, G., Banerjee, P.K. (2007) Mechanism of *tert*-butylhydroperoxide induced cytotoxicity in U-937 macrophages by alteration of mitochondrial function and generation of ROS. *Toxicol. In vitro 21,* 846-854.

12. Wefers, H., and Sies, H. (1983) Hepatic low-level chemiluminescence during redox cycling of menadione and the menadione-glutathione conjugate: relation to glutathione and NAD(P)H:quinone reductase (DT-diaphorase) activity. *Arch. Biochem. Biophys. 224*, 568-578.

13. Bruch, J., Rehn, S., Rehn, B., Borm, P. J. A., and Fubini, B. (2004) Variation of biological responses to different respirable quartz flours determined by a vector model. *Int. J. Hyg. Environ. Health 207*, 1-14.

14. Donaldson, K., and Borm, P.J. (1998) The quartz hazard: a variable entity. *Ann. Occup. Hyg. 42*, 287-294.

15. Fubini, B. (1998) Surface chemistry and quartz hazard. *Ann. Occup. Hyg. 42*, 521-530.

16. Vallyathan, V. (1994) Generation of oxygen radicals by minerals and its correlation to cytotoxicity. *Environ. Health Perspect. 102*, 111-115.

17. Schins, R.P., Knaapen, A.M., Cakmak, G.D., Shi, T., Weishaupt, C., and Borm, P.J. (2002) Oxidant-induced DNA damage by quartz in alveolar epithelial cells. *Mutat. Res. 517*, 77-86.

18. Elias, Z., Poirot, O., Daniere, M.C., Terzetti, F., Marande, A.M., Dzwigaj, S., Pezerat, H., Fenoglio, I., and Fubini, B. (2000) Cytotoxic and transforming effects of silica particles with different surface properties in Syrian hamster embryo (SHE) cells. *Toxicol. In Vitro 14*, 409-422.

19. Kim, K.A., Kim, Y.H., Seok Seo, M., Kyu Lee, W., Won Kim, S., Kim, H., Lee, K.H., Shin, I.C., Han, J.S., Joong Kim, H., and Lim, Y. (2002) Mechanism of silica-induced ROS generation in Rat2 fibroblast cells. *Toxicol. Lett. 135*, 185-191.

20. Deshpande, A., Narayanan, P.K., and Lehnert, B.E. (2002) Silica-induced generation of extracellular factor(s) increases reactive oxygen species in human bronchial epithelial cells. *Toxicol. Sci. 67*, 275-283.

21. Persson, H.L. (2005) Iron-dependent lysosomal destabilization initiates silica-induced apoptosis in murine macrophages. *Toxicol. Lett. 159*, 124-133.

22. Riganti, C., Gazzano, E., Polimeni, M., Costamagna, C., Bosia, A., and Ghigo D. (2004) Diphenyleneiodonium inhibits the cell redox metabolism and induces oxidative stress. *J. Biol. Chem. 279*, 47726-47731.

23. Gaetani, D.G., Parker, J.C., and Kirkman, H.N. (1974) Intracellular restraint: a new basis for the limitation in response to oxidative stress in human erythrocytes containing low activity variants of glucose-6-phosphate dehydrogenase. *Proc. Natl. Acad. Sci. USA 71*, 3584-3587.

24. Luzzatto, L., and Afolayan, A. (1968) Enzymic properties of different types of human erythrocyte glucose-6-phosphate dehydrogenase, with characterization of two new genetic variants. *J. Clin. Invest. 47*, 1833-1842.

25. Aust, A.E., and Eveleigh, J.F. (1999) Mechanisms of DNA oxidation. *Proc. Soc. Exp. Biol. Med. 222*, 246-252.

26. Gazzano, E., Foresti, E., Lesci, I.G., Tomatis, M., Riganti, C., Fubini, B., Roveri, N., and Ghigo, D. (2005) Different cellular responses evoked by natural and stoichiometric synthetic chrysotile asbestos. *Toxicol. Appl. Pharmacol. 206*, 356-364.

27. Riganti, C., Aldieri, E., Bergandi, L., Tomatis, M., Fenoglio, I., Costamagna, C., Fubini, B., Bosia, A., and Ghigo, D. (2003) Long and short fiber amosite asbestos alters at a different extent the redox metabolism in human lung epithelial cells. *Toxicol. Appl. Pharmacol. 193*, 106-115.

28. Hardy, J.A., and Aust, A.E. (1995) Iron in asbestos chemistry and carcinogenicity. *Chem. Rev. 95*, 97-118.

29. Fenoglio, I., Prandi, L., Tomatis, M., and Fubini, B. (2001) Free radical generation in the toxicity of inhaled mineral particles: the role of iron speciation at the surface of asbestos and silica. *Redox Rep. 6*, 235-241.

FIGURE LEGENDS

Figure 1. Effect of quartz particles on LDH release into the extracellular medium (panel A) and on the production of thiobarbituric acid-reactive substances (TBARS) (panel B) in MH-S cells. Cells were incubated for 24 h in the absence (0, control) or presence of 2.5, 5, 10, 20, 40, 80 μg/cm^2 pure quartz. Measurements were performed in duplicate, and data are presented as means ± SD (n = 3). Panel A: vs ctrl * $p < 0.005$, ** $p < 0.0001$. Panel B: vs ctrl * $p < 0.0001$.

Figure 2. Induction of apoptosis by pure quartz in MH-S cells. Cells were incubated for 24 h in the absence or presence of 20 or 80 μg/cm^2 pure quartz. The fluorescence of cell-associated annexin V-FITC and propidium iodide (PI) was measured as described in the Experimental Procedures section. Results are expressed as percentage increase of fluorescence versus the respective control incubated without quartz (assumed as 100%). Measurements were performed in duplicate, and data are presented as means ± SD (n = 3). Vs ctrl: * $p < 0.01$, ** $p<0.001$.

Figure 3. Effect of quartz on PPP activity in MH-S cells. Cells were incubated for 1, 3, 6, 24 h in the absence (ctrl) or presence of 20 (Qz 20) or 80 (Qz 80) μg/cm^2 pure quartz, without (PPP - MEN, panel A) or with (PPP + MEN, panel B) 100 μM menadione. Measurements were performed in duplicate, and data are presented as means ± SD (n = 3). Vs ctrl PPP - MEN: * $p < 0.01$, vs ctrl PPP + MEN: ***** $p < 0.0001$.

Figure 4. Effect of quartz on the activity of G6PD and 6PGD in MH-S cells. The whole cells were incubated for 24 h in the absence (0, control) or presence of 20 or 80 μg/cm^2 pure quartz, then lysed and

the enzyme activity was measured in the lysate. Measurements were performed in duplicate, and data are presented as means ± SD (n = 3). Vs ctrl: * $p < 0.0001$.

Figure 5. Effect of quartz on the activity of G6PD and 6PGD in MH-S cell lysates. Cell lysates were incubated for 4 h in the absence (0, control) or presence of either 100 or 400 μg/ml pure quartz, with (+GSH) or without (-GSH) 0.5 mM GSH. Measurements were performed in duplicate, and data are presented as means ± SD (n = 3). Vs ctrl: * $p < 0.0001$.

Figure 6. Effect of quartz on the activity of purified G6PD. Purified G6PD was incubated in cell-free conditions for 4 h in the absence (0, control) or presence of either 100 or 400 μg/ml pure quartz, with (+GSH) or without (-GSH) 0.5 mM GSH. Measurements were performed in duplicate, and data are presented as means ± SD (n = 3). Vs ctrl: * $p < 0.0001$.

Figure 7. Effect of quartz on the activity of GAPDH and LDH in MH-S cell lysates (GAPDH lys, LDH lys) and on the activity of purified GAPDH and LDH (GAPDH pur, LDH pur) in cell-free conditions. Cell lysates or purified enzymes were incubated for 4 h in the absence (0, control) or presence of either 100 or 400 μg/ml pure quartz. Measurements were performed in duplicate, and data are presented as means ± SD (n = 3).

Figure 8. Effect of quartz on the intracellular levels of glutathione (GSH) and glutathione disulfide (GSSG) in MH-S cells. Cells were incubated for 24 h in the absence (0, control) or presence of either 20 or 80 $\mu g/cm^2$ pure quartz. Measurements were performed in duplicate, and data are presented as means ± SD (n = 3). Vs ctrl: * $p < 0.0001$.

Figure 1.

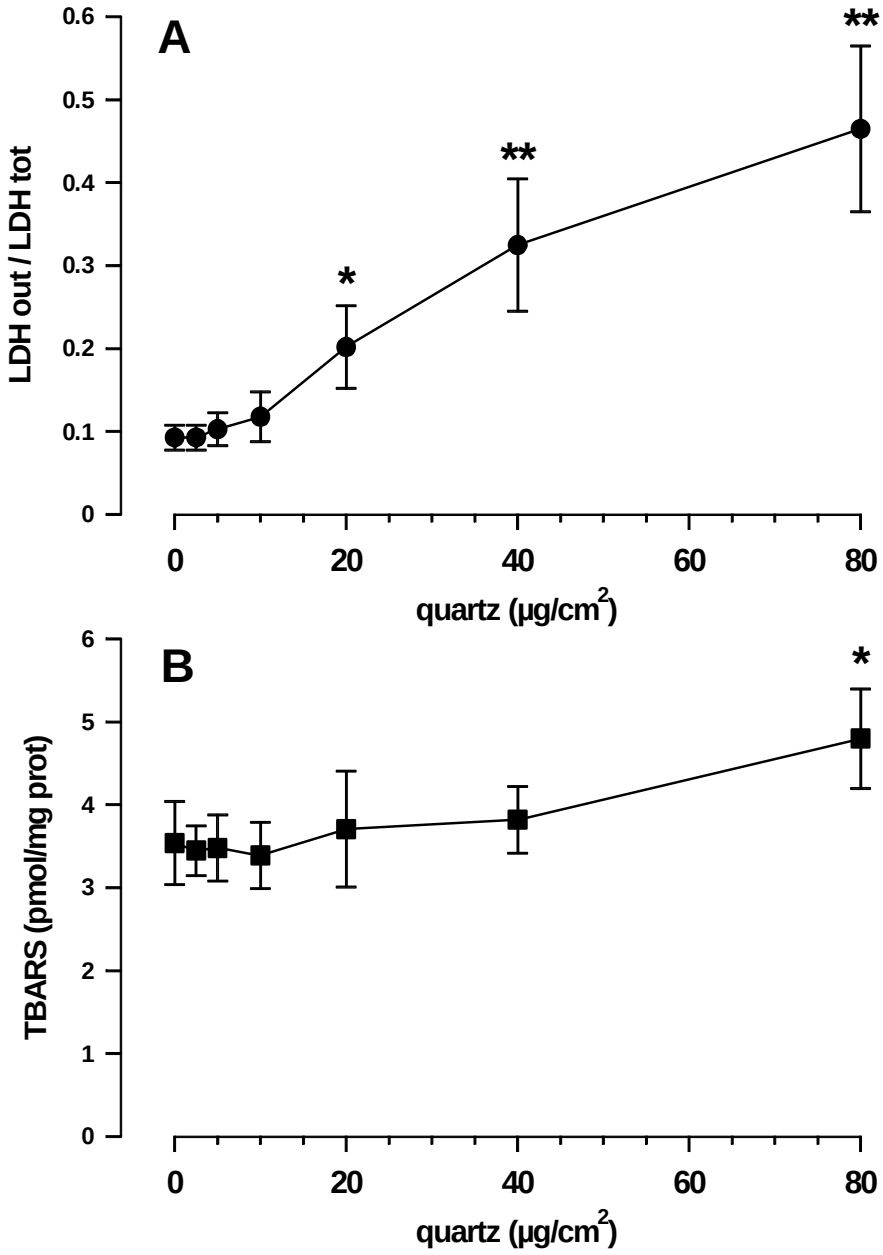
A
LDH out / LDH tot
0.6
0.5
0.4
0.3
0.2
0.1
0
*
**
**
0
20
40
60
80
quartz (µg/cm2)
B
TBARS (pmol/mg prot)
6
5
4
3
2
1
0
*
0
20
40
60
80
quartz (µg/cm2)

Figure 2.

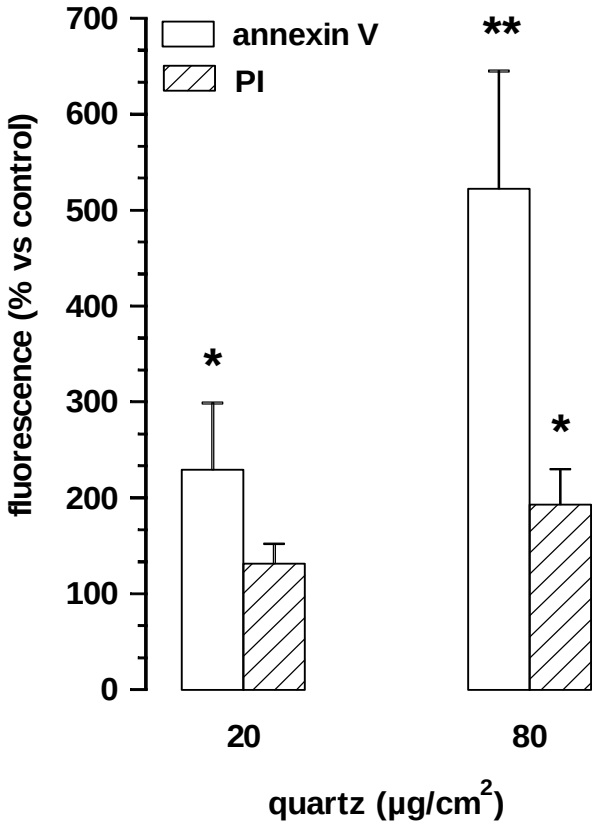
700
600
500
400
300
200
100
0
fluorescence (% vs control)
annexin V
PI
**
*
*
20
80
quartz (µg/cm2)

Figure 3.

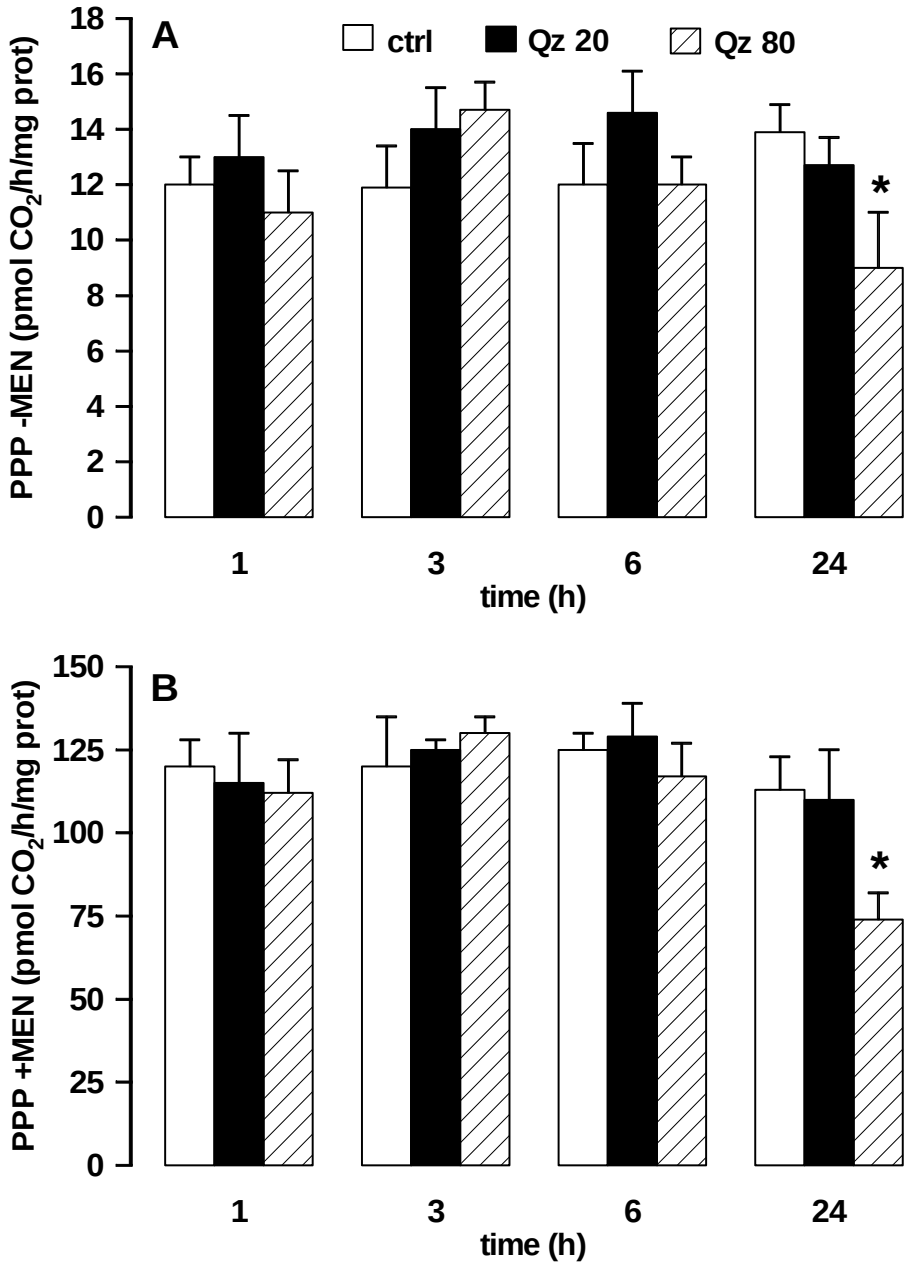
A
ctrl
Qz 20
Qz 80
PPP -MEN (pmol CO_2/h/mg prot)
18
16
14
12
10
8
6
4
2
0
1
3
6
24
time (h)
*
B
PPP +MEN (pmol CO_2/h/mg prot)
150
125
100
75
50
25
0
1
3
6
24
time (h)
*

Figure 4.

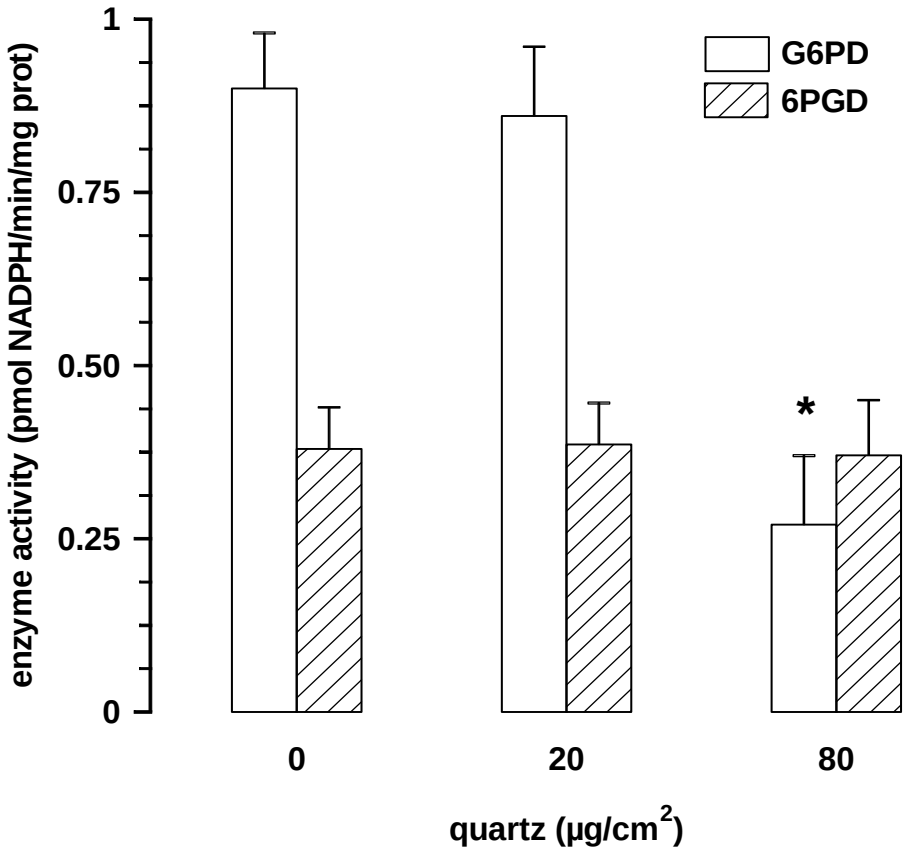
enzyme activity (pmol NADPH/min/mg prot)
1
0.75
0.50
0.25
0
G6PD
6PGD
*
0
20
80
quartz (µg/cm2)

Figure 5.

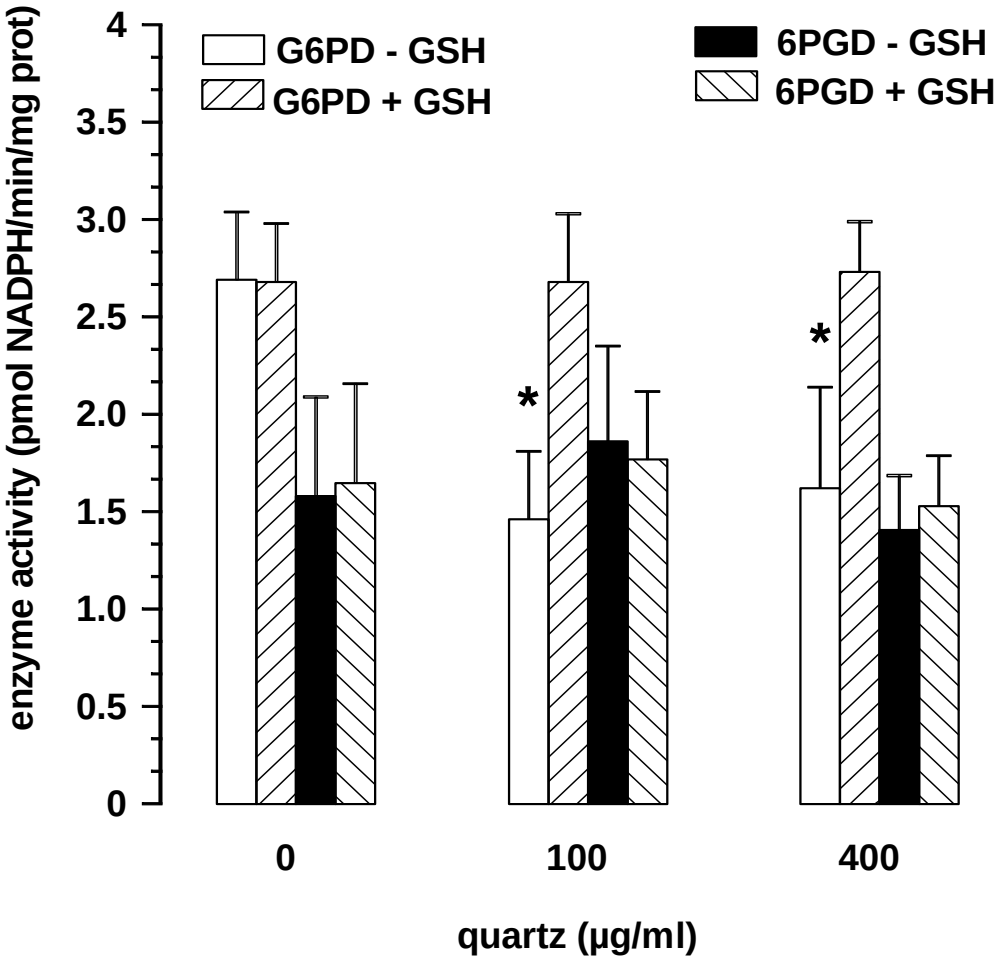
G6PD - GSH
G6PD + GSH
6PGD - GSH
6PGD + GSH
enzyme activity (pmol NADPH/min/mg prot)
4
3.5
3.0
2.5
2.0
1.5
1.0
0.5
0
*
*
0
100
400
quartz (µg/ml)

Figure 6.

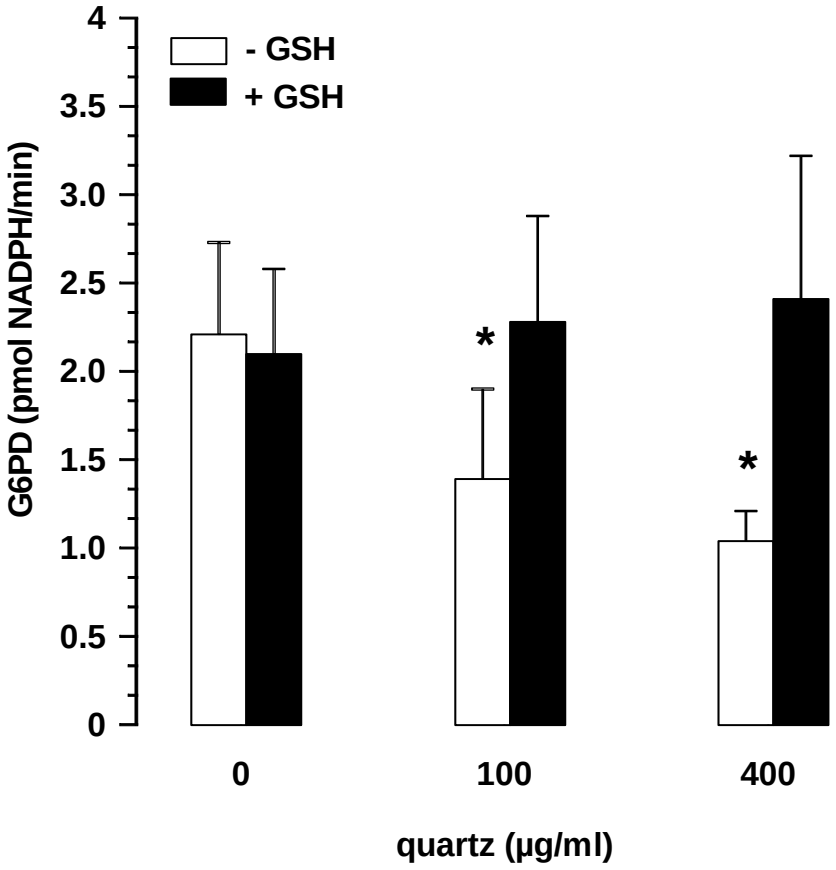
- GSH
+ GSH
G6PD (pmol NADPH/min)
4
3.5
3.0
2.5
2.0
1.5
1.0
0.5
0
*
*
0
100
400
quartz (µg/ml)

Figure 7.

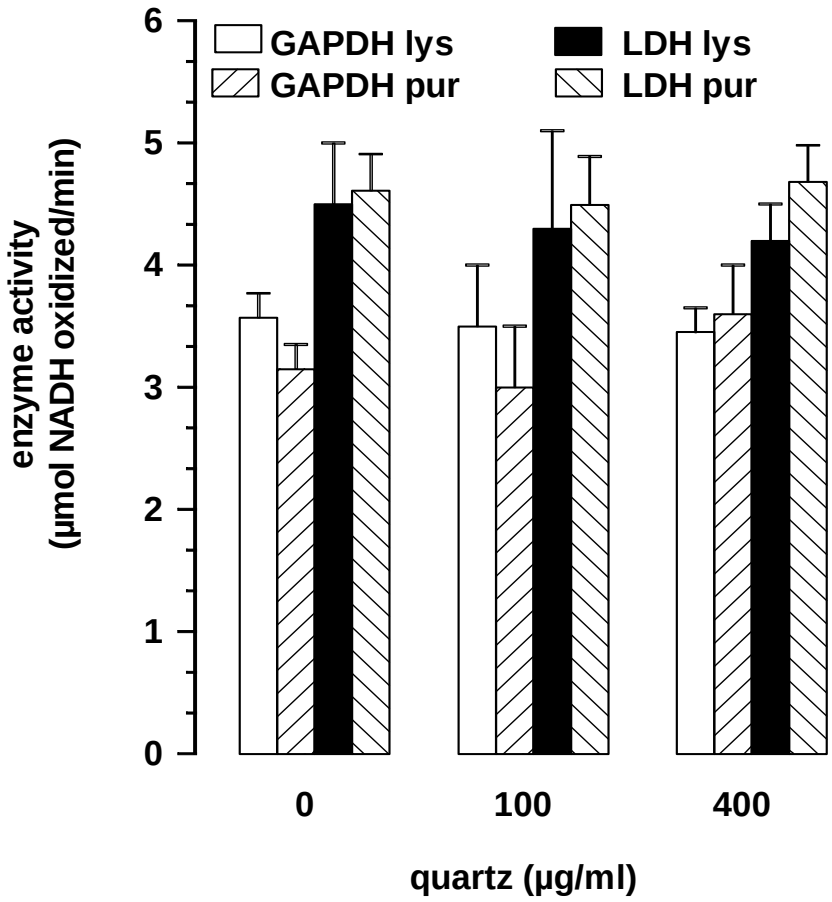
GAPDH lys
GAPDH pur
LDH lys
LDH pur
enzyme activity
(µmol NADH oxidized/min)
0
1
2
3
4
5
6
0
100
400
quartz (µg/ml)

Figure 8.

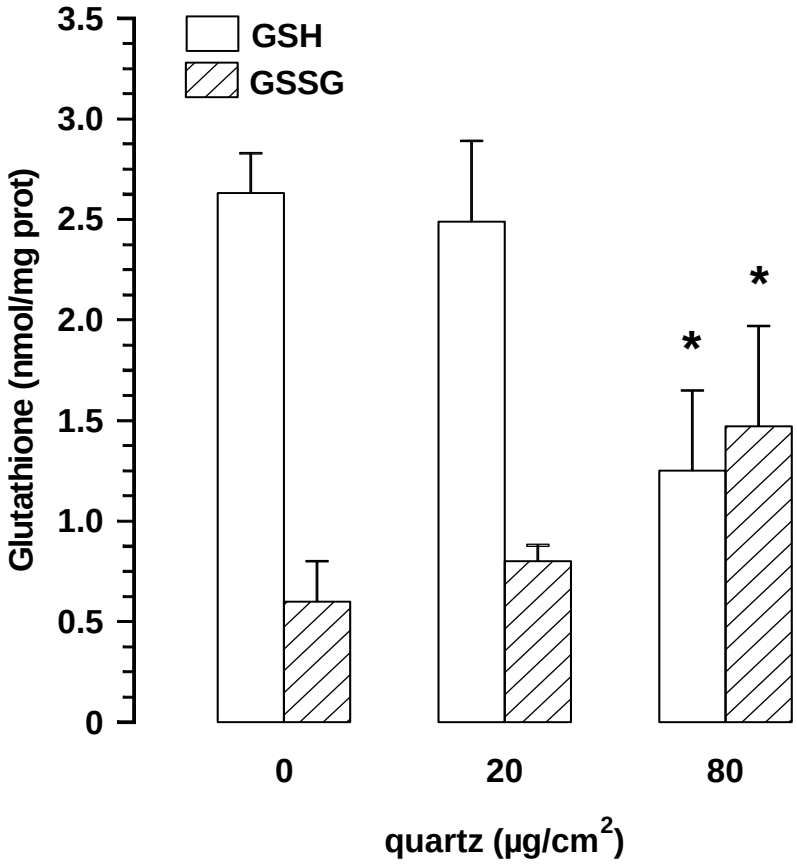
GSH
GSSG
Glutathione (nmol/mg prot)
3.5
3.0
2.5
2.0
1.5
1.0
0.5
0
*
*
0
20
80
quartz (µg/cm2)